Journal of Pharmaceutical Sciences 000 (2021) 1–15

Contents lists available at ScienceDirect

Journal of Pharmaceutical Sciences

journal homepage: www.jpharmsci.org

Pharmacokinetics, Pharmacodynamics and Drug Transport and Metabolism

Pharmacological, Pharmacokinetic, Pharmacodynamic and Physicochemical Characterization of FE 205030: A Potent, Fast Acting, Injectable CGRP Receptor Antagonist for the Treatment of Acute Episodic Migraine

Karthik Srinivasan*, Kirk Kozminski, Ying Zhang, Kazimierz Wisniewski, Trudy Kohout, Halina Wisniewska, Geoffrey Harris, Beatriz Lindstrom, Diane Hargrove

Ferring Research Institute, Ferring Pharmaceuticals, 4245 Sorrento Valley Blvd, San Diego, CA 92121, United States

ARTICLE INFO

Article history:
Received 19 April 2021
Revised 27 June 2021
Accepted 29 June 2021
Available online xxx

Keywords:
Calcitonin gene-related peptide
PK/PD
Preformulation
Human effective dose
Migraine
Allometry
Bioanalytical
LC/MS
Pharmacokinetics
Pain
CGRP
Peptide

ABSTRACT

The neuropeptide calcitonin gene-related peptide (CGRP) is known to play a central role in the underlying pathophysiology of migraine. In comparison to the effective triptan class of antimigraine treatments, the CGRP antagonists possess a comparable efficacy but a superior cardiovascular safety profile in patients. This paper describes the development of selective and potent peptidic CGRP antagonist, FE 205030, that has a fast onset of action and an optimal half-life (subcutaneous T_{max} ~ 60 min, and $t_{1/2}$ ~ 4.4 h in 80 kg pigs, respectively), which is key to prevention of the progression of debilitating migraine symptoms. The *in vivo* efficacy of this agent has been established a translational pharmacodynamic model (inhibition of capsaicin-induced increase in skin blood flow) in cynomolgus monkeys and shows maximal inhibitory activity at circulating concentrations of 30-100 nM. Antagonist activity of FE 205030 was characterized on CGRP-induced vasodilation in isolated human mesenteric resistance arteries in an *ex vivo* isometric myograph study, and FE 205030 effectively blocked CGRP-induced vasodilation with a pA_2 of 9.3 ± 0.1, mean ± standard error. Multispecies allometric scaling and modeling of subcutaneous (SC) effective concentrations indicates that a dose of 10 −30 mg/day is sufficient to achieve a drug exposure/target coverage of 8h, which is useful to prevent migraine recurrence in patients. The molecule also possesses appropriate physicochemical properties that allows for a convenient dosing form factor of 1 ml injection volume with a sufficient solubility and acceptable short-term stability, optimal for treatment of acute migraine episodes in patients. Hence, FE 205030 may provide an important fast-acting injectable option for patients suffering from frequent acute migraine episodes, complementary to preventative monoclonal antibodies and oral small molecule CGRP-R antagonist therapies.

Introduction

Calcitonin gene-related peptide (CGRP) is a 37 amino acid peptide member of the Calcitonin family.[1] The gene family is comprised of adrenomedullin, adrenomedullin 2 (intermedin) and amylin, in addition to the calcitonin gene. There are two major CGRP isoforms, the α and βCGRP, which are coded by separate genes.[2,3] The human versions of α and βCGRP share a ~90% sequence homology as they differ only in 3 amino acids.[4] While they are principally expressed in different regions in the body, αCGRP in the central and peripheral nervous system and βCGRP mainly in the enteric nervous system, it is unsurprising that they share similar biological activity due to this high structural homology.[5] CGRP's biological action is produced by agonizing the CGRP receptor (CGRP-R), a member of the G-protein coupled receptor family (G protein G_s), which activates adenylate cyclase subsequently resulting in the generation of intracellular cyclic adenosine monophosphate (cAMP).[6] CGRP binds to the receptor formed by two subunits: calcitonin receptor-like receptor (CLR) and receptor activity-modifying protein 1 (RAMP1).[7] CGRP is known to be involved in the neurotransmission of pain and is the most potent vasodilatory agent known.[8] Its circulating levels are elevated during migraine attacks and the introduction of exogenous CGRP induces migraine-like headaches in human volunteers.[9] The causative role of CGRP in migraine was first postulated in 2002 when human αCGRP (2 ug/ml) was infused IV in 12 patients for

* Corresponding author.
E-mail address: ksrca@yahoo.com (K. Srinivasan).

https://doi.org/10.1016/j.xphs.2021.06.034
0022-3549/

20 min, who then developed symptoms of migraine without aura.[10] It is also known that CGRP receptor activation results in initiation of cortical spreading depression and, finally, triptans (5-HT_{1B1D} receptor agonists) are known to prevent release of CGRP and are effective anti-migraine therapeutics.[11]

CGRP was discovered in the early 1980s.[9,12] By the late 1980s, enough was known that CGRP was postulated to play an important role in the development of migraine and was proposed as a potential drug target.[13] By the early 1990s, there was sufficient data to suggest its role in pain transmission and vasodilation to support this hypothesis and various researchers and companies began investigating peptide CGRP antagonists as potential therapeutics.[14]

The structure of α and βCGRP has been studied and has been identified as having 4 functionally relevant domains. The first few amino acids (1–7) constitute the receptor activation region, the amino acids 8–18 the first receptor binding region, the amino acids 19–27 the hinge region and the last domain of amino acids, 28–37, constitute the second receptor binding regions. Hence, the first pharmacological tool used to probe this system was the truncated peptide CGRP (8–37), which was relatively potent but was not selective against the CGRP-R. Typically, the lack of potency and/or unfavorable PK prevented peptide antagonists from advancing to the clinic and eventually research efforts concentrated on small molecules and monoclonal antibody approaches.[14–20]

In the mid-2000s, a variety of small molecule CGRP antagonists entered clinical development, namely: olcegepant (BIBN4096BS), telcagepant (MK-0974), MK-3207, MK1602, BMS-694153, BMS-927711 and BI44370TA, MK-8825, BMS-742413, thiazolidinones, tyrosine surrogates and polyethylene glycolated (PEGylated) peptides.[21] The most studied compounds of this class are called the 'gepants,' for example, olcegepant and telcagepant. Olcegepant was the first to enter the clinic and demonstrated robust and rapid efficacy with an improved adverse event (AE)/tolerability profile compared to the well-established triptan class of drugs typically used for treating acute migraine. The key proof-of-concept study with olcegepant involved a double-blind, randomized, placebo-controlled design, in which the drug was administered intravenously (10 min infusion) at doses of 0.25–10 mg to patients suffering from an acute migraine attack.[14,22] Superiority of olcegepant to placebo was demonstrated with respect to several primary and secondary end points, including reduction in pain from 'moderate to severe' to 'mild to moderate', pain freedom and relief of nausea, photophobia, and phonophobia.[14,22] While demonstrating high potency and efficacy, olcegepant required IV administration and possessed poor physicochemical properties.[20] Olcegepant, due to its poor physicochemical characteristics and its high molecular weight (869.6 Da), was found to possess low oral bioavailability and was discontinued in favor of a second-generation molecule with more favorable physicochemical properties.[23] However, this second-generation molecule was eventually found to be somewhat less potent than expected, had evidence of mild liver enzyme elevation in one patient in phase II and was shown to be a potent CYP3A4 inhibitor. These factors potentially contributed to its discontinuation as well.

Telcagepant (MK-0974) was one of several small molecule CGRP antagonist compounds advanced into clinical trials.[14] This molecule showed promise in several large, phase III, randomized, placebo controlled trials with efficacy very similar to triptans and a much more favorable AE and tolerability profile.[21] Telcagepant trials also demonstrated the cardiovascular safety of CGRP antagonism in patients with coronary artery disease and that telcagepant was generally well tolerated for acute intermittent migraine treatment in these patients.[24] Trials were also performed to investigate if telcagepant could also be used as a migraine prophylaxis with twice daily (BID) dosing of the drug for 12 weeks. While the data suggest a potential role for CGRP receptor antagonism in migraine prophylaxis, the observed aminotransferase elevations did not support the use of telcagepant for daily prophylactic administration.[25] More recently, two gepants, rimegepant, and ubrogepant, have undergone large Ph III clinical trials and have recently been approved by the FDA for acute treatment of episodic migraine, based on data presented for 2 primary end points: 2 h pain freedom and 2 h freedom from the most bothersome symptom (MBS), both of which had statistically significant reduction in the trials (amongst positive outcomes in other secondary end points). The efficacy of these two agents seems lower than rizatriptan and hence the clinical utility of gepants for acute treatment is likely to be first in patients with known vascular risk factors, due to the fact that the gepants seem safer than triptans in this patient population.[11]

In addition, lasmiditan represents a new class of recently approved, orally active, antimigraine agents (also called ditans) which shows a favorable safety and efficacy profile. Ditans are selective 5-HT_{1F} receptor agonists and were developed based on the rationale that most triptans activate trigeminal 5-HT_{1F} receptor which is hypothesized to be responsible, at least in part, for the triptans' antimigraine pharmacology.[26] With respect to safety, lasmiditan has shown to not constrict human coronary arteries while being effective in the treatment of migraines. The site of action of his drug is not fully known, but due to its high inherent lipophilicity it is likely that it can act directly on central descending antinociceptive pathways. Also, since 5-HT_{1F} receptors are located on trigeminal fibers, there is a possibility that lasmiditan could favorably modulate CGRP release in the CNS.[26]

In addition to the small molecule CGRP antagonists, four antibody based CGRP antagonist molecules are in Phase III clinical development or have been approved (Eptinezumab/ALD403, Fremanezumab/TEV48125, Galcanezumab/LY2951742, Erenumab/AMG334). The first three of these agents are humanized mAbs targeting the CGRP ligand and the last is a fully human mAb against the CGRP receptor. As opposed to the gepants, which have been studied for both acute and prophylactic migraine treatment, CGRP mAbs have only been investigated for the prevention of episodic and chronic migraine, and episodic and chronic cluster headache.[24] In contrast to the small molecule antagonists, the antibodies are targeted at treating chronic migraine as the modality inherently permits longer exposures, which in turn helps reduce the overall frequency of migraine attack in patients with chronic migraine (more than 14 attacks per month). Most of the antibody clinical trials indicate an efficacy in the line of reduction in 2 headaches per month after 9–12 weeks of treatment.[24] These results demonstrate that CGRP mAb is relatively safe and well tolerated for chronic migraine and is suitable for further clinical evaluation.[27] While this is serves a different migraine patient population as compared to a small molecule or peptide based therapeutic, the data continues to support the utility and safety of the CGRP-R target mechanism of action.

Based upon the established clinical efficacy associated with this target, coupled with expected improved safety and tolerability profiles compared to the triptan class of anti-migraine products, we present in this publication a peptidic CGRP antagonist discovery program. Initial reports of such peptidic efforts were published in early 1998/2006 (Beck-Sickinger et. al.) where peptides were designed based on CGRP (27–37).[25,28] This was followed in 2008 by design of potent and selective agents with suitable metabolic stability by a different group of researchers.[29] Subsequently, cyclic peptidic antagonists were designed with hCGRP cAMP antagonist kb ~0.03 nM based on the fragment FVPTNVGSKAF.[30]

Revisiting an injectable peptide approach would confer a very fast onset of action and most of the advantages of the small molecule CGRP antagonists, with the exception of the convenience of oral dosing. It would also help develop molecules with very high potency and selectivity and good physicochemical properties in order to develop a

convenient injectable product for treatment of acute episodic migraine. It would also eliminate the non-mechanistic metabolic toxicity exhibited by some small molecule antagonists (given the distribution and metabolic fate of peptides is fundamentally different and that they generally do not have liver toxicology issues observed sometimes in the small molecule drugs). Most importantly, based on the significantly improved clinical efficacy of injectables (with fast onset of action) like sumatriptan as compared to their oral counterparts, an injectable CGRP antagonist could provide superior and sustained pain relief over oral small molecule CGRP antagonists.[31]

The discovery program was built with the belief that a successful product would preferably be a low volume, highly soluble, subcutaneously delivered injection. This necessitates a highly potent compound with favorable physicochemical properties, allowing formulation via the envisaged mode, as compared to reference peptidic agents in the literature (FE 992325 or Eli Lilly CGRP antagonist and FE 992326 or human aCGRP (8–37), details in the Chemicals and Reagents section). In addition, an ideal agent would require a duration of action similar to the triptans and small molecule CGRP antagonists. Most importantly, such an agent should possess a rapid onset of action to address the underlying cause of the disease within minutes of dosing to prevent symptoms worsening and avoid protracted suffering in patients.

Based upon extensive evaluation of efficacy vs. exposure for both the triptan, ditans and small molecule CGRP antagonists, we believe that the peptidic product should be therapeutically efficacious for at least 3 hours and up to 6-8 hours; a longer duration would confer little if any advantage. Indeed, in the triptan class, there are a wide variety of products with substantially different elimination kinetics. In this group, there are hints that there may even be reduced overall utility of a product with a very long exposure as it may increase the risk for rebound migraine headaches.[31] In summary, our product profile is a highly potent, selective peptidic CGRP receptor antagonist; a combination of pharmacological, physicochemical and pharmacokinetic properties that enable a small volume (1 mL or less) injectable product, a agent having a rapid onset of action and with an ideal duration of response between 3 and 8 h.

Materials and methods

Chemicals and reagents

FE 205030 (Oxazole-2-carbonyl-D-Val-Phe(2-Cbm)-c(Cys-Orn (iPr)-Asp-Val-Gly-Pro-Phe-Cys)-3Pal- NH_2) shown in Fig. 1, FE 992325 (Eli Lilly CGRP Antagonist, 4-F-Bzl)-(D-Val)-Tyr-cyclo [Cys-Agp-Asp-Val-Gly-Pro-Phe-Cys]-3Pal-NH_2):, FE 992326 (human-αCGRP(8-37)-NH_2 Antagonist, H-Val-Thr-His-Arg-Leu-Ala-Gly-Leu-Leu-Ser-Arg-Ser-Gly-Gly-Val-Val-Lys-Asn-Asn-Phe-Val-Pro-Thr-Asn-Val-Gly-Ser-Lys-Ala-Phe-NH_2) and olcegepant were synthesized in Ferring Research Institute Inc. (purity >99%), MK-3207 and telcagepant were obtained from MedChem Express.

Equipment, instruments, and software

Instech Autosampler Unit (Instech; ABS2), Autosampler software: ABS212 Software Version 2.13, Beckman Coulter Allegra® X-15R Benchtop Centrifuge, VETEQUIP COMPAC^5 Inhalation Anesthesia Systems Mobile Anesthesia Machine, vortexer mixer VWR multi-tube vortexer, Mettler Toledo analytical MTS microbalance, liquid handler- Hamilton Microlab Star, ABSciex API 5000 LC/MS/MS system were used in laboratory wet experiments.

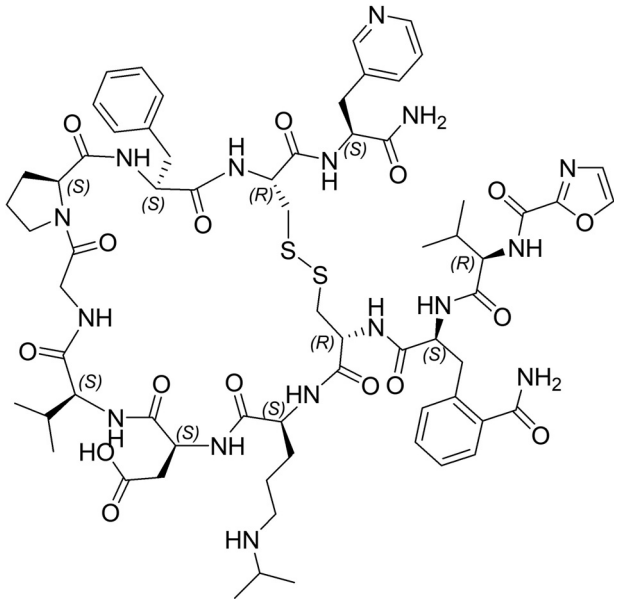

Figure 1. The chemical structure of FE 205030.

Thermodynamic solubility and stability assessment

Solubility measurement

Small-scale/volume (~200 uL) concentrated solutions were prepared at 25, 50 and 150 mg FB/mL (using a miniPrep^{TM} filtration vial) in order to minimize the use of API for preliminary solubility assessments. In each experiment, API was weighed directly into the vial, followed by addition of the aqueous vehicle/buffer. The vial was capped with the accompanying plunger unit, which was then depressed to reduce the internal volume of the vial. The mixture was immediately subject to moderate shaking for 16–20 h at room temperature with the aid of a titer plate shaker. At the end of the shaking period, the plunger unit was fully depressed to the bottom to filter and separate any undissolved material. An aliquot of the recovered solution/supernatant was sampled and quantitated using calibration standards and HPLC/UV methods.

Stability Assessment: FE 205030 at a concentration of 25 mg free base (FB)/mL was prepared in 25 mM Acetate Buffer (pH 4.5). An aliquot of the freshly prepared sample solution was diluted to 0.5 mg/mL and analyzed by HPLC. The rest sample solution was sealed tightly and stored at room temperature for one month and then reanalyzed by HPLC.

Aggregation Investigation: FE 205030 was tested for its potential to form aggregates after formulating at concentrations of either 25 or 50 mg FB/mL.

Representative bioanalytical method for FE 205030

For PK sample analysis, 50 ul of plasma samples were transferred into a clean 96-well plate. For preparation of calibration and QC samples, first working standards solution in solvent was prepared at concentration 20x higher than the intended plasma concentration (WSTD: 5–10,000 ng/ml). These working standards were then diluted 20x using plasma (2.5 uL of working stock spiked on to 47.5 ul of plasma and vortexed). Then 30 ul of internal standard was added to 50 ul of plasma samples such that final concentration of analog internal standard in each sample was 10 ng/ml, prior to protein precipitation and subsequent sample processing. The next steps in sample processing involved addition of 150 μL of acetonitrile to all wells followed by vortexing on multi-tube shaker. The plates were

then centrifuged at 5700 rpm for 30 min. A volume of 200 uL of supernatant was transferred to a clean plate, concentrated to dryness under nitrogen, reconstituted with 100 μL of 20% mobile phase B Buffer, vortexed for 5 minutes and centrifuged at 5700 rpm for at least 30 min again prior to injection into the LC–MS/MS system for analysis.

The LC/MS/MS system consisted of Shimadzu pump (Kyoto, Japan) LC-30AD HPLC, and Sciex QTRAP 5500 mass spectrometer (Toronto, Canada) with Turbo V™ Ion Source. The representative assay for FE 205030 is described below: Phenomenex Aeris Wide Pore 3.6u XB –C18 from Phenomenex Inc. (Milford, MA) was the chromatographic column utilized. The injection sample volume was 40 μl and the assay run time was 5 min. The chromatographic mobile phase A was 0.01% TFA in Water and the mobile phase B was 0.01% TFA in 70% Acetonitrile. The LC method used a flow rate of 0.5 ml/min with mobile phase B at 5% for 0.2 min; to 10% at 0.5 min; to 20% at 0.9 min; to 50% at 2.8 min; followed by washing the column at 100% mobile phase B for 1 min (till time 3.8 min) and finally reequilibrating the column at 5% mobile phase B for ~0.5 min (till 5 min end time). The MS/MS transition used for FE 205030 was m/z 713 (doubly charged precursor ion) to 704 Da (product ion, dwell time 100 msec). The electrospray source was operated at a source temperature of 500°C, with a capillary voltage of -4500 V and CAD gas set at pressure of 10 psi; the precursor ion fragmentation occurred at collision energy of -22 eV. The transitions (precursor to product) for the compounds were optimized to achieve their highest respective sensitivity conditions.

Chromatograms were integrated using Sciex Analyst v1.6 software and the data uploaded into Watson LIMS 6.4 for regression analysis. A weighted $1/x^2$ linear regression analysis was conducted, where x is the concentration of analyte. The dynamic range of the assays was in the range of 0.25–500 ng/ml and multiple levels of quality control samples (in plasma) were utilized to qualify each run in the program.

In every run, appropriate blanks, control blanks and carry-over blanks were used to characterize the potential contamination, cross-talk, background (matrix related interferences) and carryover during the course of the entire 96-well sample analysis runs.

In vivo pharmacokinetic experiments

Rat IV and SC PK studies

Rodent studies were conducted at Ferring Research Institute according to local Animal Care and Use Policies & Procedures. Male Sprague– Dawley rats weighing 250–300 g were purchased from Charles River Laboratories (Hollister, CA) with jugular vein and carotid artery cannula (IV groups) in place. Animals were allowed to acclimate for 3–4 days before study initiation with free access to food and water at all times prior to dose administration. IV and SC dose administration were given under a parallel study design to each group of animals. Compounds FE 992325 and FE 992326 were dosed 0.3 mg/kg IV and 1 mg/kg SC, respectively. FE 205030 was dosed 0.2 mg/kg IV and 0.6 mg/kg SC, respectively. Doses were administered using a standard vehicle of 5% mannitol and a nominal dose volume of 1 mL/kg. A total of n = 4 rats were used for each study dosing route. Following IV or SC administration, 250 μl blood was withdrawn in collection tubes with EDTA K_2 anticoagulant from the carotid artery cannula (CAC) from each animal (one sample/time point) at times listed in Table 3. Samples were collected with an automated blood sampler (ABS2) from Instech Laboratories and samples were maintained at 4°C for the length of the study and then processed to retrieve plasma from whole blood. At the completion of the study, plasma samples were stored at -20°C until analyzed by LC/MS/MS bioanalytical method described in the previous section.

Minipig IV, SC PK and injection site reaction studies

The purpose of this study was to obtain the pharmacokinetic parameters and perform visual macroscopic evaluations for injection site reactions in minipigs. Studies were conducted at Sinclair Research (Auxvasse, MO). The animals were acclimated for a minimum of 1 day prior to initial dose initiation. FE 205030 was nominally dosed at 0.1 mg/kg and 0.25 mg/kg by IV and SC, respectively. The vehicle used in the IV study was 5% mannitol in water. The dosing solution used in the SC study was 50 mM acetate buffer pH 5.0 made isotonic with mannitol (2.8%), where a 20 mg/ml solution of FE 205030 was administered SC at a volume of ~1 ml/injection. The animals weighed approximately 80 kg. A group of n = 4 miniature pigs (male castrated double ported animals) were used in each leg of the study. The animals had chronic vascular access ports (VAPs) implanted for dose administration via the portal vein, and another for systemic blood collection via the iliac vein. IV doses were administered via a temporary percutaneous catheter in either a cephalic or saphenous vein. Each animal was assigned to the study based on acceptable health as determined by the attending veterinarian following a prestudy health evaluation, which included serum chemistry and hematology evaluations as well as a physical exam. All animals were fasted overnight prior to each dosing session and food was returned approximately 2–3 h post dose. There was a washout period of 7 days between each dosing session. Immediately following IV dosing, the dosing catheter and/or VAP was flushed with 3 mL saline. For both routes, blood samples (1 mL whole blood, K_3EDTA anticoagulant) were collected via the chronic venous catheter and subcutaneous VAP, or by venipuncture of a femoral vein if the chronic catheter had lost patency. IV blood samples were collected at 3, 5, 10, 20, 30, 45, 60, 90, 120, 180, 240 min following dosing. SC blood samples were collected at 5, 10, 20, & 40 min, and 1, 1.5, 2.5, 3.5, 4.5, 6, 8 and 24 h post-dose. The blood tubes were then inverted multiple times, centrifuged at ~3000 rpm for ~15 min, at ~4 °C, and then the plasma removed and placed into a cryovial for storage at -70°C until bioanalysis.

Study of injection site reaction: FE 205030 was formulated for this study at a concentration of 20 mg/mL and dosed at a volume of 1 mL per animal using a vehicle that contained 50 mM acetate buffer (at pH 5.0) with added mannitol to maintain isotonicity. FE 205030 was thus injected at relevant human doses (drug concentrations, volumes and buffers mentioned above) subcutaneously. Test material was dosed SC behind the left or right ear. Clinical observations were made prior to each dose administration, and then at 0.25, 0.5, 1, 2, 6, and 24 hours post dose. Dosing sites and overlaying skin was monitored closely after injection for signs of adverse injection site reactions. This involved visual observation of the injection site for transient irritant type reaction, which include tenderness, warmth, or redness at the injection site. Any observation of blistering, bleeding, formation of scab, infection or symptoms/behaviors indication that the animal was suffering pain was to be recorded as a serious injection side reaction. Animals displaying such serious reactions were euthanized, tissues collected, and histology of the injection site performed for further investigation based on the severity of the observation.

Monkey IV PK study

FE 205030 was nominally dosed at 0.1 mg/kg (n = 4) and FE 992325 was dosed at 0.2 mg/kg (n = 3) both in 5% mannitol to male, cynomolgus non-human primates. In addition to aiding characterization of PK of FE205030 in non-human primate to support allometric scaling and human CL predictions, this data was important for ascertaining doses and exposures for supporting a monkey pharmacodynamics assessment, as described in later sections.

Studies were conducted at Sinclair Research (Auxvasse, MO) using young adult male cynomolgus monkeys (average weight 6.2 kg). The animals had chronic vascular access ports (VAPs) implanted for for

systemic blood collection via the iliac vein. IV doses were administered via a temporary percutaneous catheter in either a cephalic or saphenous vein. Each animal was assigned to the study based on acceptable health as determined by the attending veterinarian following a prestudy health evaluation, which included serum chemistry and hematology evaluations as well as a physical exam. All animals were fasted overnight prior to each dosing session and food was returned approximately 2–3 h postdose. Immediately following dosing, the dosing catheter and/or VAP was flushed with 3 mL saline. Blood samples (1 mL whole blood, K_3EDTA anticoagulant) were collected via the chronic venous catheter and subcutaneous VAP, or by venipuncture of a femoral vein if the chronic catheter had lost patency. Blood samples were collected at 3, 5, 10, 20, 40, 60, 90, 120, 180, 240, and 360 min for FE 205030 or at3, 5, 10, 20, 30, 45, 60, 90, 120, 180 and 240 min for FE 992325 following dosing. Plasma processing was conducted as described earlier for the rat and minipigs studies.

PK data analysis

Pharmacokinetic analysis was performed using WinNonlin™ Professional Version 3.1 (Pharsight Corporation, Mountain View, CA) and Watson LIMS (NCA, Thermo Lab Systems Inc.). The actual times of blood draw were utilized for the pharmacokinetic analysis. Pharmacokinetic parameters were calculated using a noncompartmental approach based on the statistical moment theory. The parameters that were calculated for FE 205030 included C_{max} (observed), $AUC_{0-\infty}$, CL, and $t_1/_2$. The bioavailability following SC administration was determined by comparing dose-normalized area under the plasma concentration-time curves for the SC and IV routes, respectively (i.e., AUC_{SC}/AUC_{IV}). Plasma concentrations of analytes below the lower limit of quantitation (LLOQ) were reported as less than LLOQ.

Plasma protein binding (PPB) method

In this study, the PPB of CGRP antagonists was measured by first preparing a working solution at a concentration of 20,000 ng FB/ml and diluting (5 uL into 495 ul of fresh rat or human plasma) to obtain quadruplicates at a final testing concentration of 200 ng FB/ml in polycarbonate thick-walled tubes. Corresponding blank samples (not spiked with analyte) were also included. All samples were incubated in the rotor inside the chamber under vacuum at 37°C for 15 min. They samples were then centrifuged at 120,000 RPM (770,000xg) at 37°C for 30 min. Under these conditions, the centrifugate partitions into three layers: the top layer contains mostly phospholipids and other lower density plasma components, a protein free middle layer that contains the unbound drug, and the bottom layer that contains the protein pellet along with the protein bound drug. The ultracentrifugation conditions, mentioned above, were optimized to achieve a near protein free middle layer while avoiding meaningful sedimentation of the unbound peptide (analyte) of interest. Upon completion of centrifugation, 50 ul of the middle layer sample of the ultracentrifuged plasma is removed from each tube. The middle layer of blank samples was then spiked to prepare standard and QC samples. Internal standard solution was then added into the PPB and standard calibration curve and QC middle layer samples. The plate with PPB, spiked calibration standards and QC samples was then processed (see bioanalysis section) for LC/MS/MS analysis and quantitation.

Data Analysis: Test compound concentrations in the middle layer PPB samples are determined from the internal standard-normalized test compound peak areas and calibration curve fitting. The middle layer sample triplicates are averaged to determine the mean unbound test compound concentration. The Percent Plasma Protein Binding (%PPB) is calculated as:

$$\%\text{PPB} = \frac{(\text{Spiked analyte concentration in plasma} - \text{Mean unbound analyte concentration})}{\text{Spiked analyte concentration in plasma}} \text{ x } 100$$

where *spiked analyte concentration in plasma* is 200 ng FB/ml and *mean unbound concentration* is the average of the compound concentration measured in the quadruplicate ultracentrifuged plasma middle layer samples.

Monkey skin blood flow PD assessment method

Animals: The data were collected using 9 (capsaicin-responding) adult male cynomolgus monkeys weighing 3.0–4.0 kg. The monkeys were used for multiple treatments with a minimum of 5 days of recovery in between experiments. The study was conducted at Covance Laboratories Inc. (Greenfield, IN). All procedures were compliant with the USDA's Animal Welfare Act (9 CFR Parts 1, 2, and 3) and the National Institutes of Health, Office of Laboratory Animal Welfare.

Compound formulation and administration: FE 205030 was formulated in normal saline (0.9% sodium chloride) on the day of administration. Capsaicin (Sigma, M2028) was formulated at 100 mg/mL in 30% ethanol (200 proof), 30% Tween 20, 40% water.

FE 205030 was administered by IV bolus followed by IV infusion at five target steady state plasma concentrations (Css) of 3, 10, 30, 100, and 300 nM. Pharmacokinetic simulations were used to calculate the IV bolus dose and infusion dose rates to achieve the target Css. Vehicle bolus (0.6 mL) and infusion rate volumes (25 ul/min) were held constant across FE 205030 dose administrations. The final intended steady state plasma concentrations (Css) of 3, 10, 30, 100, and 300 nM were mostly achieved in vivo, as shown in Table 7.

In-life experimental protocol: The experimental protocol timeline is depicted in schematic in Fig. 10. The experiment involved topical application of capsaicin within 2 rubber O-rings placed on the forearm of the monkeys. Ring 1 was used to determine the capsaicin-control response for each monkey on each experimental day during IV infusion of vehicle, and Ring 2 was used to determine the effect of FE 205030 or vehicle administration (IV) on capsaicin response.

On each experimental day, animals fasted overnight were anesthetized (10 mg/kg intramuscular ketamine), intubated, and delivered 0.75–1.5% isoflurane via trachea tubes for the duration of the experiment. Cutaneous hair was removed from the ventral side of one forearm. The animals were placed on a warm surgical blanket and the shaved arm placed on a circulating water heating pad. After acclimation for approximately 20 min, 2 rubber O-rings (8 mm, termed Ring 1 and Ring 2) were placed on each animal's forearm in an area absent of visible major vessels. Saphenous vein catheters were then set to enable IV administration of treatment.

Vehicle was administered (IV bolus/IV infusion) and 25 min later a baseline measurement for skin blood flow within Ring 1 was obtained by laser Doppler imaging (LDI: MoorLDI, LDI2-IR with software v2). 5 min after baseline measurement, capsaicin (2 mg in 20 μL) was applied topically to the skin within Ring 1. Skin blood flow within Ring 1 was measured every 5 min through 30 min post-capsaicin after which infusion of vehicle was stopped. Ring 1 is considered the capsaicin-control.

After completion of measurements on Ring 1 (capsaicin control), administration of treatment, FE 205030 or vehicle, was initiated (IV bolus followed by IV infusion for a total of 70 min). At 25 min post

Table 1
Assessment of solubility (mg FB/mL) of FE 205030 in acetate buffer.

Formulation Concentration (mg/ml)	Buffer pH	Buffer Strength (mM)	Mannitol Added (%)	Measured Concentration (mg/ml)
25	4.5	25	4.1	23.7
50	4.5	50	2.8	48.3
150	5.0	100	none	137

initiation of treatment, a baseline measurement for skin blood flow within Ring 2 was obtained. 5 min after Ring 2 baseline measurement, capsaicin (2 mg) was topically applied to the skin within Ring 2. Skin blood flow within Ring 2 was measured by LDI every 5 min through 30 min post-capsaicin.

Blood samples (K_3EDTA, femoral vein) for compound plasma concentration determination were collected following the final skin blood flow measurement, and again 10 min later. Plasma was prepared from whole blood. After the final blood sample, infusion of treatment was stopped, animals recovered from anaesthesia and were returned to the colony.

Doppler data analysis: Raw data from laser Doppler imaging were captured on Moor LDI software. In each image file, the position of the rubber O-ring on the animal forearm was used to define the area of interest for determination of average flux statistics (in perfusion units, arbitrary units based on Doppler shifts) as a measurement of skin blood flow.

Skin blood flow (SBF) in Ring 1 and Ring 2 at each time point post-capsaicin administration were reported as percent change from baseline in the corresponding Ring, calculated as follows:

$$\textbf{SBF change from baseline}\ (\%) = \frac{\text{SBF at time x (Ring 1 or Ring 2)} - \text{SBF baseline (Ring 1 or Ring 2)}}{\text{SBF baseline (Ring 1 or Ring 2)}} \text{ x } 100$$

Statistical analyses were performed using SAS version 9.2. A mixed linear analysis of variance was used to test for differences between the repeated measures of Skin Blood Flow Change from Baseline (%) in Ring 2 and Ring 1 for the various treatments. The fixed factors in the statistical model were treatment group, time, and treatment by time interaction. The animal was the random factor in the model. $P < 0.05$ were considered significant.

Ex vivo human skin studies

Ex vivo antagonism of αCGRP-induced vasodilation in isolated human mesenteric resistance arteries was evaluated by isometric wire myograph (DMT Multi myograph system) and data was collected continuously using Notocord-hem. Human mesentery tissue collected from 11 donors was obtained from Stemgent-Asterand (Cambridge, MA). Briefly, human mesenteric resistance arteries were dissected under stereomicroscope while bathed in carbogen-aerated physiological saline solution (PSS: 119.8 mM NaCl, 4.6 mM KCl, 1.5 mM NaH_2PO_4, 0.7 mM Na_2HPO_4, 11.5 mM D-glucose, 25 mM $NaHCO_3$, 2.4 mM $CaCl_2$, 1.2 mM $MgCl_2$, pH 7.35-7.45). Multiple segments were collected from the same artery to allow for paired test and control segments. Arterial segments (2 mm) were mounted in isometric wire myograph systems with tissue baths containing aerated PSS maintained at 37°C. Passive length-tension relationships were determined for each arterial segment and used for artery normalization by stretching. Arterial contractility was stabilized by potassium-induced depolarization with three consecutive exposures to a high potassium solution (124 mM K^+ PSS). Vessel segments were then contracted by bathing in 40 mM K^+ PSS. Once contraction stabilized, arterial segments were tested for αCGRP-induced relaxation in cumulative concentration response manner in presence or absence of single concentrations of FE 205030. Control segments were run for each artery; a time-control segment receiving only the contractile agent (40 mM K^+ PSS), and a paired-control segment receiving the contractile agent and αCGRP dose response assessment in the absence of FE 205030. Each vessel segment was tested only once.

Results

Solubility and stability

The aqueous solubility concentrations were chosen keeping in mind the anticipated human doses (<100 mg), desired dosing volumes (<1 ml), which translated into a peptide concentration in the ranges tested and described below. As described in Table 1, when a freshly prepared (and 16–24 h room temperature shaken) 25, 50 and 150 mg FB/ml solution of FE 205030 in acetate buffer was filtered and assayed, a supernatant concentration of 23.7, 48.3 and 158 mg FB/mL was determined respectively. This is within the assay's experimental margin of error and so the formulated concentration is considered fully thermodynamically soluble at these target concentrations. After initial formulation and shaking (16–20 h), the solution was also noted as visually clear and fluid with no observable change in viscosity.

The stability sample solution prepared at 25 mg FB/mL in 25 mM acetate buffer (pH 4.5) remained visually clear and with no observable change in viscosity after one-month storage at room temperature. However, it was noticed that compound purity dropped from initial 99.8–98.1% based on HPLC analysis, indicating that the compound might undergo a slight degradation process.

Bioanalytical results

Bioanalysis of peptides was conducted using a protein precipitation, gradient chromatography, positive mode electrospray ionization LC/MS/MS method using close structural analogs of analytes as internal standards. Representative calibration curves, chromatograms (LLOQ, ULOQ and blanks) and IS performance of FE 205030 are shown in Figs. 2–4 respectively. The corresponding assay performance (accuracy and precision) data is presented in Table 2. The precision of the method (expressed as %CV) was shown during method qualification to be in the range of 0.793 to 2.52%. The accuracy of the method (expressed as %Error) was found in the range of -1.33 to -6.11%). The assay calibration curve from plasma also routinely showed R^2 values of >0.99. The double blank samples (and predose samples) did not show any significant matrix related interference peaks and the control blank samples did not indicate the presence of interfering peaks from the analog internal standards in the LC/MS/MS method(s) used. The carryover blanks placed after the ULOQ samples showed an assay carryover of <20% of the LLOQ peak area in most instances, indicating overall a very reliable LC/MS/MS bioanalytical method.

FE 205030 and literature CGRP antagonists comparative pharmacokinetics

Rat PK: The IV and SC PK of FE 992326 (CGRP (8-37)), FE 992325 (literature reported peptidic CGRP antagonist) and the clinical

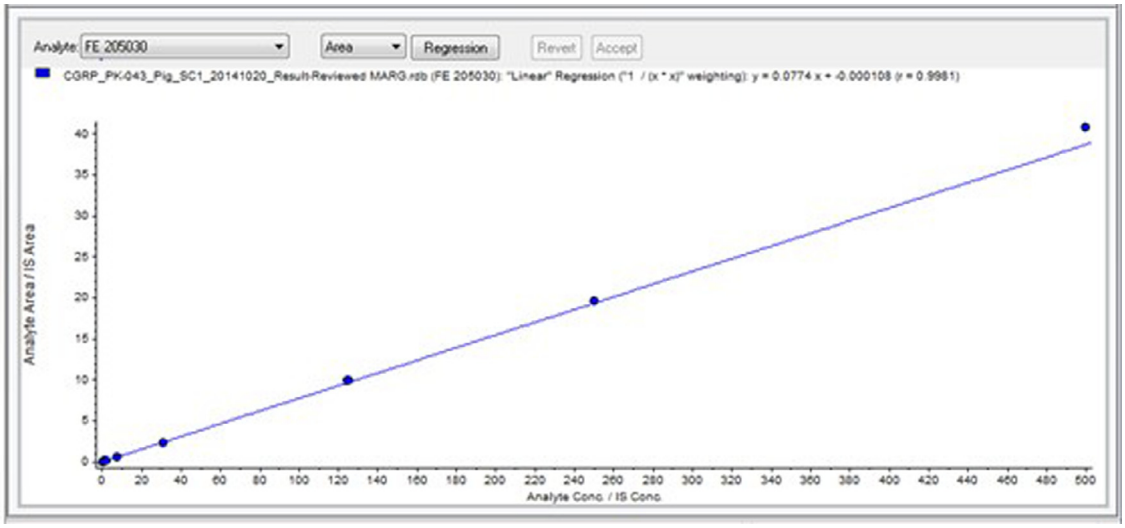

Figure 2. Representative calibration curve data from assay characterization of FE 205030 from minipig plasma. The R^2 value for this bioanalytical run is 0.9981.

Figure 3. Representative FE 205030 Study A. Double Blank, LLOQ, ULOQ Chromatograms.

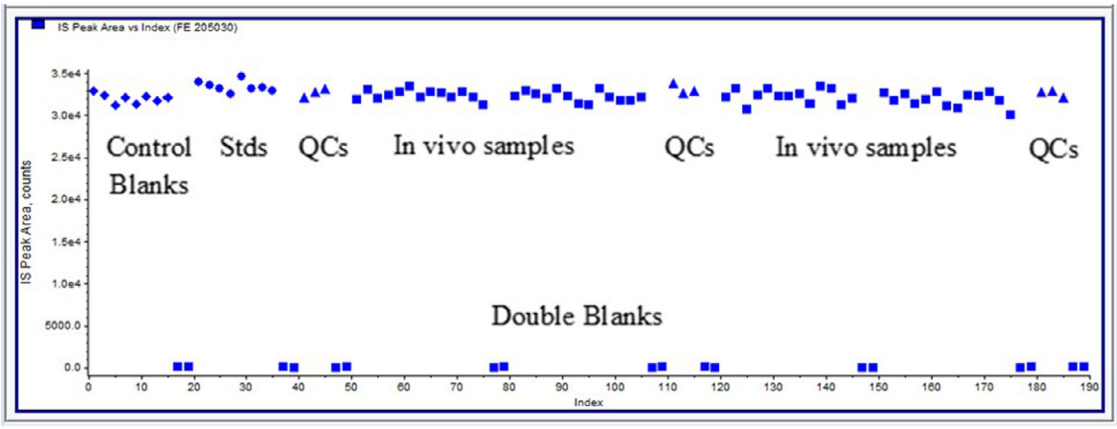

Figure 4. Representative analog internal standard performance in the assay.

candidate FE 205030 were dosed as described in the methods section. As shown in Table 3 and Fig. 5, it was observed that FE 205030 had lower systemic clearance (8.54 ml/min/kg) comparable to the kidney glomerular filtration rate in adult rats (~9 ml/kg/min). In comparison, FE 992326 and FE 992325 had appreciably higher clearance of 109 and 13.7 ml/kg/min, respectively. The terminal half life of FE 205030 (25.1 min) was also longer than the above-mentioned comparator analogs (FE 992326: 6.44 min; FE 992325: 21.04 min). The volume of distribution of FE 205030 (Vdss: 251 ml/kg) indicated that the peptide was largely restricted to the extracellular fluid and with limited tissue distribution. FE 205030 showed much greater subcutaneous bioavailability of 97% versus 8% for FE 992326 and 36% for FE 992325.

Minipig PK: FE 205030 was dosed to 4 male Yucatan miniature swine (80–88 kg) via IV and SC routes. As shown in Table 4 and Fig. 6, the primary PK parameters of FE 205030 following single IV dose were: systemic clearance (CL) 1.33 ml/kg/min, elimination half-life ($t_{1/2}$) 82 min and volume of distribution at steady state (Vdss) 110 ml/kg. Clearance value following single SC dose was similar to that of IV administration. Subcutaneous bioavailability was 100% whereas the SC terminal half-life (264 min) was longer than that of IV indicating protracted subcutaneous absorption. As shown in Fig. 6 (comparative minipig IV and SC PK profiles of FE 205030), the exposure and duration of action of FE 205030 in minipigs, assuming translation to humans, is expected to cover the needed duration of action in migraine patients.

No transient irritant-type reaction was observed during the course of the above experiments, which include tenderness, warmth, or redness at the injection site.

Monkey PK: In addition to aiding characterization of PK of FE 205030 in non-human primate to support allometric scaling and human CL predictions, these data were important for ascertaining doses and exposures for supporting a monkey pharmacodynamics assessment, as described in later sections. Male cynomolgus macaques (4.8–7.5 kg) were dosed with FE 205,030 (n = 4) and literature reference CGRP antagonist FE 992326 (n = 3) via IV route. As shown in Table 5 and Fig. 7, and similar to observations in rats, FE 205030 showed lower systemic clearance than FE 992325 (2.4 vs 6.3 ml/kg/min).

Allometric scaling: Using systemic clearance values obtained from rats (0.36 kg), monkey (6.3 kg), and mini pig (85 kg), an

Table 2
Representative calibration and QC sample results for analysis of plasma samples of FE 205030 in Male Yucatan Mini Swine.

Standard #	Calibration Concentration (ng FB/ml)	Found Concentration (ng FB/ml)	% Found
1	0.49	0.504	2.9
2	0.98	0.905	-7.7
3	1.95	2.06	5.6
4	7.81	7.35	-5.9
5	31.3	29.7	-5.1
6	125	129	3.2
7	250	254	1.6
8	500	526	5.2

FE 205030 Intra-Run QC	QC Low ng FB/ml	QC Medium ng FB/ml	QC Highng FB/ml
1	1.47	27.4	200
2	1.45	28.8	192
3	1.45	28.3	200
Nominal Concentration (ng FB/ml)	1.50	30.0	200
Observed mean (ng FB/ml)	1.46	28.2	197
S.D. (ng FB/ml)	0.01	0.71	4.62
Precision (%CV)	0.793	2.52	2.34
Accuracy (%Error)	-2.89	-6.11	-1.33

Table 3
Plasma pharmacokinetic parameters of FE 992326, FE 992325 and FE 205030 in **Male Sprague–Dawley Rats** following IV or SC administration (N = 4).

Peptide (Dose) IV	FE 992326 (0.3 mg/kg) CGRP (8-37)	FE 992325 (0.3 mg/kg) (Eli Lilly Ref)	FE 205030 (0.2 mg/kg)
C_0 (ng/ml)	698 ± 121	2298 ± 254	1380 ± 173
$AUC_{0-\infty}$ (ng.min/ml)	2939 ± 97	23670 ± 3787	23800 ± 3250
CL (ml/kg/min)	109 ± 5	13.8 ± 2.0	8.5 ± 1.2
$t_{1/2}$ (min)	6.5 ± 1.8	21± 2	25 ± 8
Vdss (ml/kg)	498 ± 69	247 ± 19	251 ± 13

SC	FE 992326 (1 mg/kg)	FE 992325 (1 mg/kg)	FE 205030 (0.6 mg/kg)
Cmax/Dose (ng/ml/mg/kg)	40.1 ± 16	184 ± 29	825 ± 151
AUC_{0-t} (ng.min/ml)	777 ± 437	25900 ± 3920	68900 ± 7660
$AUC_{0-\infty}$ (ng.min/ml)	879 ± 503	29200 ± 4380	69100 ± 7620
CL/Fsc (ml/kg/min)	1770 ± 1280	39 ± 7	8.8 ± 1.0
$t_{1/2}$ (min)	11 ± 8.4	48 ± 11	23 ± 2
t_{max} (min)	7.6 ± 2.9	56 ± 26	90 ± 0
Fsc (%)	8.48 ± 4.78	35 ± 5	97 ± 11

Mean ± S.D.; IV Timepoints (min) for FE 992326 and FE 992325: 2, 6, 10, 15, 20, 30, 45, 60, 90, 120, IV Timepoints (min) for FE 205030: 2, 6, 10, 15, 20, 40, 60, 90, 135, 180; SC Timepoints (min) for FE 992326 and FE 992325: 5, 10, 20, 30, 45, 60, 90, 120, 180, 240, 300, SC Timepoints (min) for FE 205030: 5, 10, 20, 40, 60, 90, 120, 180, 240, 300.

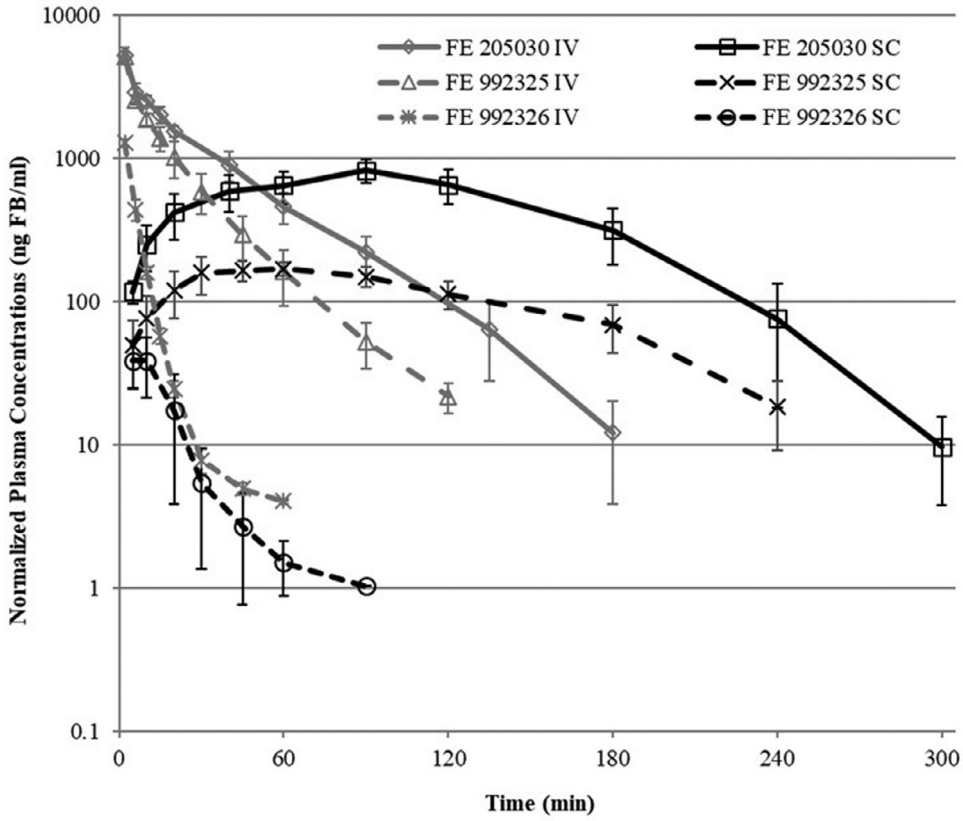

Figure 5. Mean plasma concentrations of FE 992326, FE 992325 and FE 205030 in male Sprague–Dawley rats following a single IV (0.3, 0.3 and 0.2 mg/kg, respectively) or SC (1, 1 and 0.6 mg/kg, respectively); dose normalized to 1 mg/kg.

allometric scaling plot was generated. As shown in Fig. 8, systemic clearances versus respective experimentally measured body weight of the three above mentioned specie showed simple allometry correlation, with a relationship shown below:

$$CL = 5.5(BW)^{0.7},\ R^2 = 0.99$$

Table 4
Plasma pharmacokinetic parameters of FE 205030 in **Male Minipigs** Following IV or SC Administration ($N = 4$).

Peptide (Dose) IV	FE 205030 (0.1 mg/kg)
C_0 (ng/ml)	2150 ± 674
$AUC_{0-\infty}$ (ng.min/ml)	76,000 ± 8580
CL (ml/kg/min)	1.3 ± 0.2
$t_{1/2}$ (min)	82 ± 9
Vd_{ss} (ml/kg)	110 ± 13
SC	**FE 205030 (0.25 mg/kg)**
C_{max}/Dose (ng/ml/mg/kg)	3148 ± 1170
AUC_{0-t} (ng.min/ml)	203,000 ± 1410
$AUC_{0-\infty}$ (ng.min/ml)	208,000 ± 6240
CL/Fsc (ml/kg/min)	1.2 ± 0.1
$t_{1/2}$ (min)	264 ± 80
t_{max} (min)	60 ± 36
F_{sc} (%)	115 ± 7

Mean ± S.D.

Plasma protein binding

The data from the study was tabulated in Table 6. The results indicate that reference peptide FE 992325 and FE 205030 had a rat PPB of 50.48 and 9.17%, respectively. A similar pattern of PPB was observed in human plasma, where the FE 992325 and FE 205030 PPB was found to be 46.1 and 16.6%, respectively.

Monkey skin blood flow PD assessment

Time courses of skin blood flow change from baseline (%) mean values for each treatment group are shown in Fig. 11 and *p*-values for statistical analysis are summarized in Table 8. The application of capsaicin within Ring 1 induced the expected increase in skin blood flow of approximately 2-fold from baseline in all treatment groups at 30 min post application. Observable and statistically significant ($P < 0.05$) differences between Skin Blood Flow Change from Baseline (%) in Ring 2 and Ring 1 were time-related and FE 205030 dose-related. Animals treated with vehicle or with FE 205030 at the lowest Css (3 nM), had similar responses in Ring 2 and Ring 1 over the time course and no significant differences (Fig. 11, Panels A and B, $P > 0.05$ Table 8). At a target Css of 10 nM and higher FE 205030 induced significant inhibition of capsaicin-induced increase in skin blood flow beginning at 15–25 min post-capsaicin application (Fig. 11, Panels C-F and Table 8).

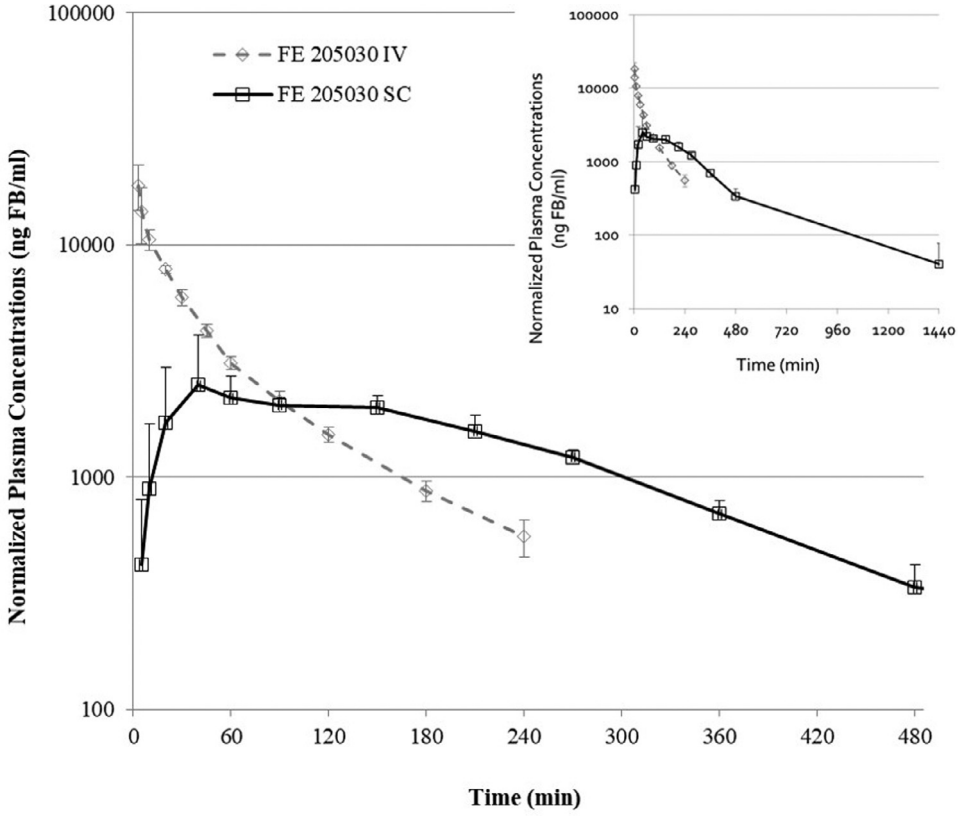

Figure 6. Mean (±SD) plasma concentrations of FE 205030 in male Yucatan miniswine following a single IV (0.1 mg/kg) or SC (0.25 mg/kg); dose normalized to 1 mg/kg. **Inset**: PK profile of FE 205030 as seen in the main plot, but the time axis extended to show up till 60 hours post SC dose.

Table 5
Plasma pharmacokinetic parameters of FE 992325 and FE 205030 in **Male Cynomolgus Monkeys** following IV administration (N = 3 for FE 992325, N = 4 FE 205030).

Peptide (Dose) IV	FE 992325 (0.2 mg/kg)	FE 205030 (0.1 mg/kg)
C_0 (ng/ml)	4760 ± 1040	1230 ± 120
$AUC_{0-\infty}$ (ng.min/ml)	31,600 ± 737	42,000 ± 7960
CL (ml/kg/min)	6.3 ± 0.2	2.4 ± 0.4
$t_{1/2}$ (min)	69 ± 7	65 ± 5
Vd_{ss} (ml/kg)	206 ± 49	177 ± 15

Mean ± S.D.

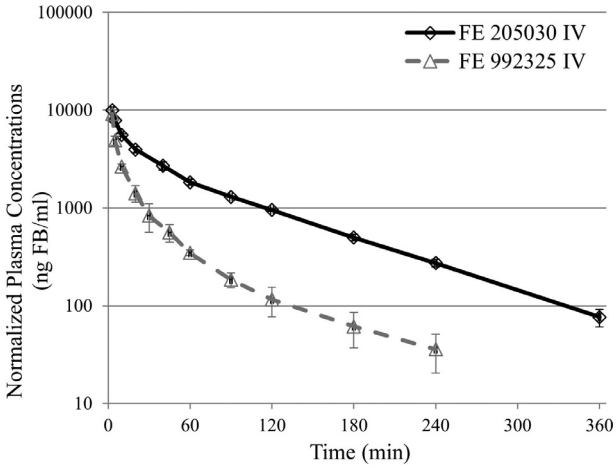

Figure 7. Mean (±SD) plasma concentrations of FE 992325 and FE 205030 in cynomolgous monkeys following a single IV (0.2 mg/kg and 0.1 mg/kg, respectively); dose normalized to 1 mg/kg.

To further illustrate the response to treatment, the paired Ring 1 and Ring 2 skin blood flow measurements from individual animals at 30 min post-capsaicin administration in each treatment group are shown in Fig. 12. Administration of vehicle (IV bolus/IV infusion) lead to a random distribution in the paired measurements at 30 min post-capsaicin application, with some Ring 2 Skin Blood Flow Change from Baseline (%) measurements being increased relative to Ring 1, and some measurements decreased relative to Ring 1. A similar random distribution also occurred in animals that received the low dose of FE 205030 (target C_{ss} 3 nM). FE 205030 administration at target C_{ss} of 30–300 nM lead to decreased Ring 2 response in comparison to the corresponding Ring 1 (capsaicin control) response in all of the treated animals. It is noted that, as shown in Table 8, as the target Css increases from 10 nM to 100 nM, statistically significance is achieved at a shorter time post capsaicin, due to higher relative plasma exposures, culminating at statistical significance being achieved at 15 min at 100 nM target Css exposure. At the highest 300 nM Css, a statistical significance was achieved only at 25 min. This departure from the general trend is probably due to the observation that the Ring 1 (capsacin control) response at 300 nM Css was almost ~50% lower than Ring 1 response at 100 nM Css, as shown in Table 12. As a matter of fact, the Ring 1 control response to capsacin was the lowest in the 300 nM Css group when compared to all the doses in the experiment. It is also important to point out that the absolute CIDV inhibition at

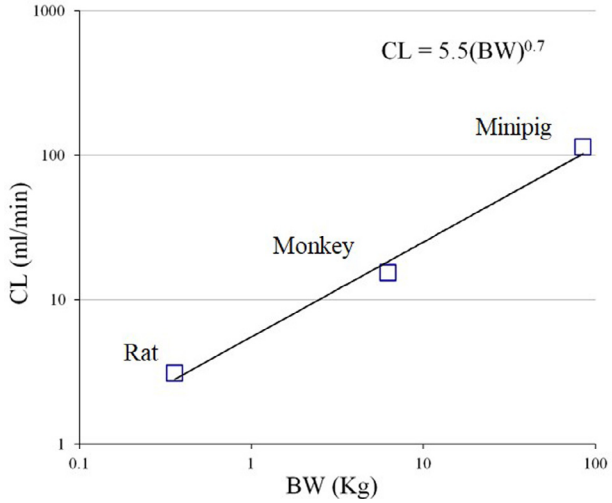

Figure 8. Interspecies allometric scaling of FE 205030 body weight (BW) versus IV clearance in rat, monkeys and minipigs

Table 6
Rat and human plasma protein binding of FE 992325 and FE 205030 measured using ultracentrifugation method.

Species	FE 992325	FE 205030
Rat (%PPB)	50 ± 5	9 ± 3
Human (%PPB)	46 ± 4	17 ± 2

Mean ± S.D.

Table 7
Compound concentrations measured in plasma (continuous sc infusion PK experiments in monkeys in support of CIDV experiments).

FE 205030	Plasma Concentration (nM)		
Target Css (nM)	Mean	STD	N
3	2.1	0.7	6
10	9.6	3.0	6
30	26	8.2	8
100	137	59	6
300	330	86	6

N: number of replicate treatments.

Table 9
Concentrations of compounds tested in the human ex vivo skin CGRP mediated vasodilatation assay.

Compound	Name	Concentration Tested (nM)
FE 205030	N/A	0.3, 1, 3 or 1, 3, 10
FE 992334	Olcegepant	1, 3, 10
FE 992379	MK-3207	0.1, 0.3, 1 or 0.1, 1, 10
FE 992384	Telcagepant	100, 316, 1000
FE 992011	human- αCGRP	0.01, 0.03, 0.1, 0.3, 1, 3, 10, 32, 100, 316, 1000, 3160

N/A: not applicable.

300 nM Css was very similar to 100 nM Css, the latter 100 nM Css which showed the best statistical response to treatment.

The measured plasma concentrations of FE 205030 were consistent with the targeted C_{ss} (Table 7). Plasma exposures, on average, were within 1.4-fold of the target values.

Ex vivo human skin studies

To evaluate the *ex vivo* effect on αCGRP-induced vasodilation, the force of contractile response was measured in isolated human mesenteric resistance arterial segments subjected to cumulatively increasing concentrations of αCGRP in the presence or absence of FE 205030.

Treatment of arterial segments with αCGRP in the absence of antagonist (paired-control segments) resulted in concentration-dependent vasodilation, as judged by reduction in the force of arterial contractile response upon exposure to increasing concentrations of αCGRP. The fitted estimate of αCGRP EC_{50} for the 18 paired-control segments tested (across all treatment groups) ranged from 0.24 – 3.8 nM, with a geometric mean of 1.4 nM (SEM = 0.23 nM). The fitted

Table 10
Antagonist activity of FE 205030 and comparator compounds on CGRP-induced vasodilation in isolated human mesenteric resistance arteries.

Compound	pA_2			
	Mean	Std. Error	(95% CI)	N
FE 205030	9.3	0.1	(9.2–9.4)	4
Olcegepant	10.7	0.3	(10.5–10.9)	6
MK-3207	9.4	0.1	(9.3–9.4)	5
Telcagepant	8.1	0.2	(7.9–8.3)	3

Std.: standard; CI: confidence interval; N: number of replicates. Standard error from fitting of data to the Gaddum/Schild EC_{50} shift model were calculated by GraphPad Prism; reported are the cumulative standard error calculated from the fitted Standard error across replicates.

Table 8
Statistical analyses testing for differences in Skin Blood Flow between Ring 2 and Ring-1 following administration of vehicle or FE 205030 at the indicated target Css in the CIDV model.

Time Post Capsaicin (min)	*P* - value Vehicle	FE 205030 Target Css				
		3 nM	10 nM	30 nM	100 nM	300 nM
5	0.633	0.484	0.297	0.645	0.651	0.299
10	0.518	0.854	0.889	0.883	0.2062	0.384
15	0.221	0.2206	0.998	0.244	0.0215*	0.633
20	0.383	0.167	0.315	0.0084*	0.0038*	0.222
25	0.886	0.426	0.0326*	0.0001*	<0.0001*	0.0117*
30	0.197	0.669	0.0048*	<0.0001*	<0.0001*	0.0023*
N	12	6	6	8	6	6

Vehicle (sterile saline) was administered (IV bolus/IV infusion) prior to the Ring 1 measurements in all treatment groups. Vehicle or FE 205030, were administered (IV bolus/IV infusion) to achieve the indicated target Css prior to the Ring 2 measurements. Capsaicin was applied to the skin within both rings. N: number of replicate treatments.

* $P < 0.05$.

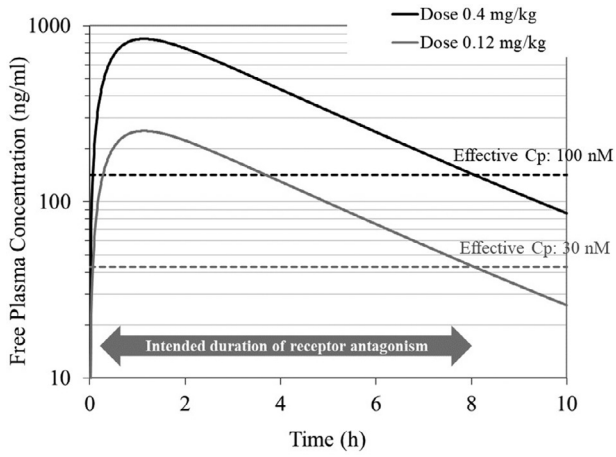

Figure 9. PK/PD simulation of potential human exposure and duration of CGRP receptor antagonism based on in vivo monkey PD data for effective Cp and simulation of SC PK.

estimate of the maximal efficacy of αCGRP (E_{max}) in the absence of antagonist ranged from 54 to 93% 40 mM K+ PSS, with a mean of 81% (SEM = 2.3%, N = 18).

Pre-treatment of arterial segments with FE 205030, olcegepant, MK-3207, or telcagepant at multiple concentrations shifted the αCGRP response to the right in a dose-related manner without depressing the E_{max} relative to that observed in the paired-control segments. Summary statistics for the pA_2 values are presented for each compound in Table 10. The pA_2 for FE 205030 (9.3 ± 0.1, mean ± standard error) was increased relative to telcagepant (8.1 ± 0.2), similar to MK-3207 (9.4 ± 0.1), and decreased relative to that of olcegepant (10.7 ± 0.3).

Discussion

Bioanalysis methods

LC/MS/MS assays were developed for the lead compound FE 205030, FE 992325 and FE 992356 from plasma matrix of multiple species as reported in the methods and section. The assays were characterized and the in vivo samples analysed with QCs showed acceptable precision and accuracy. The calibration curves were linear with R^2 values >0.99 in most instances. Hence, the bioanalytical method and the PK data shown in the paper are reliable and reproducible and reflect the true disposition of CGRP antagonists in various preclinical species shown.

Solubility and stability

The purpose of the experiment was to characterize the equilibrium solubility (also known as thermodynamic or shake-flask solubility) of FE 205030 and the solution stability in the pH 4.5 acetate buffer, which is the anticipated dosing formulation in the clinic. Solubility values were measured at various concentration levels (25 −100 mg FB/mL) after overnight shaking (16−20 h) at room temperature. In this type of assay, a known amount of solid compound is continuously shaken against a known volume of liquid in a sealed vessel at room temperature for a pre-determined amount of time. The concentration of dissolved contents is then determined by measuring the concentration of drug in solution using techniques such as high performance liquid chromatography with ultraviolet light detection (HPLC-UV).

Although traditional equilibrium solubility is a well-established assay, it can consume large amounts of peptide, especially when assessment of high solubility ranges (mg/mL) is desired. Hence, a modification to the traditional protocol involving the use of Mini-UniPrep™ self-filtering incubation vials was adopted. These vials offered several advantages over traditional approach including a) wide opening for easier compound dispensing, b) adjustable internal volume via a movable plunger apparatus, c) good liquid movement against solid compound, even at low volumes, and d) built-in filtering mechanism for easier recovery of dissolved contents. Thus the use of Mini-UniPrep filtration vials is essential for reducing compound requirements while screening for high solubility. Results from this assay were useful for identifying and prioritizing high-solubility compounds, developing structure-solubility relationships, and for determining formulation feasibility in desired vehicles.

Solutions prepared at 25 mg FB/mL in pH 4.5 acetate buffer were stored at room temperature in a sealed vial, and they were monitored visually over a period of one month. Although there was no visible aggregation and viscosity increase observed, FE 205030 solution was found to undergo a slight degradation during storage. Further

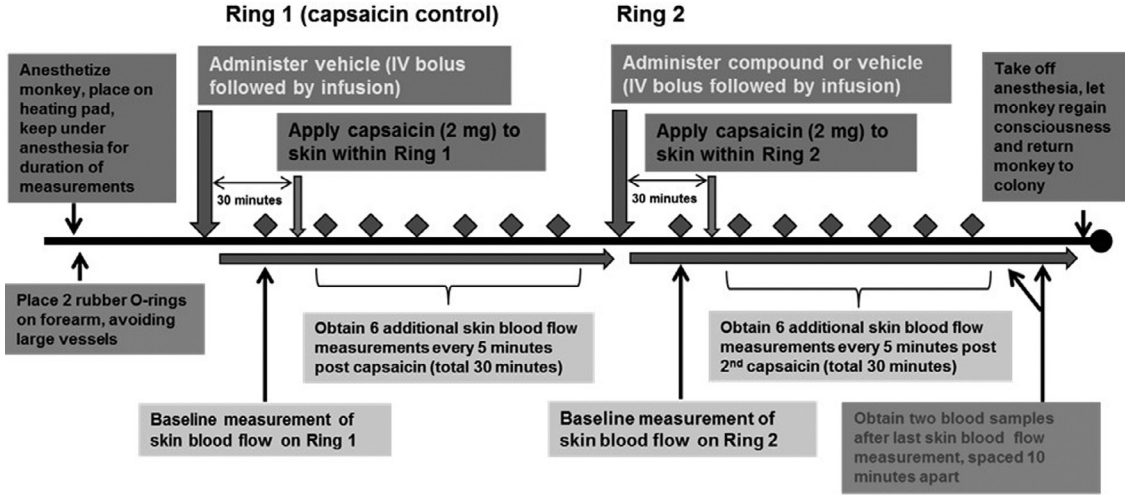

Figure 10. Protocol depiction for the capsaicin-induced dermal vasodilation assay in monkeys.

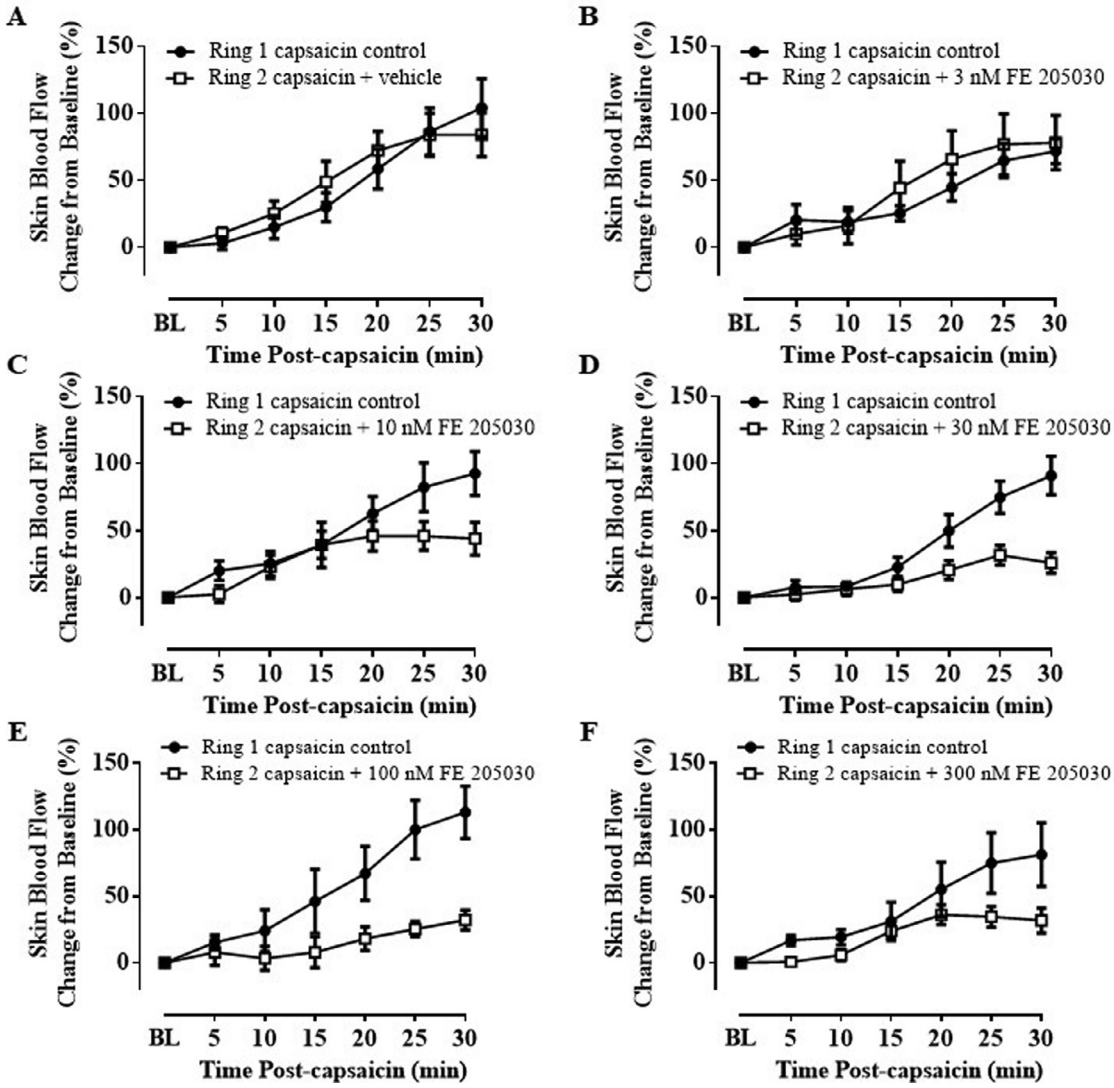

Figure 11. Effect of vehicle or FE 205030 on skin blood flow in cynomolgus monkey CIDV model. Time course of the percent change from baseline in skin blood flow at the site of capsaicin application as determined by LDI. Shown are mean ± SEM from 6–12 replicates for each treatment group; Ring 1: capsaicin + vehicle for all treatment groups(capsaicin control) and Ring 2: capsaicin + vehicle or FE 205030 at the indicated target Css. Error bars which are not visible are encompassed within the symbol. BL: baseline.

investigation revealed that the major degradant for FE 205030 in aqueous solutions was a hydrolysis product with a mass difference of +18 as a result of cyclic peptide ring open. Therefore, a freshly prepared solution is preferred in future experiments. More extensive stability assessment and formulation development will be required as the program advances to the development stage.

Plasma protein binding

The binding of drugs to proteins in plasma (PPB) can affect the disposition (clearance) of the drug, transport across cell membranes and binding to tissues (biophase), which in turn affects the pharmacodynamics response. Even though PPB does not affect the AUC_{free} or average free plasma concentration for drugs predominantly cleared by the hepatic route ,[32] it is important to incorporate PPB into assessment of peptidic drug candidates as they are predominantly cleared by nonspecific proteases (in tissue and in circulation) and through renal excretion.

Proteins in plasma and tissue can reversibly bind drug molecules and affect pharmacokinetics, whole-body distribution and, as a result, interaction with the therapeutic target in the tissue, especially for non-hepatically cleared peptidic drugs. It is understood that techniques which use membranes for *in vitro* plasma protein binding measurement, such as equilibrium dialysis and ultrafiltration, are more suitable for smaller molecules of less than approximately 500 Da and less suitable for larger molecules, mostly due to nonspecific biding and limitations in membrane pore size to accommodate molecules with higher hydrodynamic radii. The purpose of our experiment was to accurately measure the *in vitro* PPB of drug candidates using an ultracentrifugation method, and the results indicate that FE 205030 has a reasonable free fraction in humans (73.4%) in comparison to the reference peptide FE 992325 (53.9%).

Ex vivo human skin studies

In an *ex vivo* isometric myograph study, the novel peptidic CGRP receptor antagonist FE 205030 effectively blocked CGRP-induced vasodilation in isolated human mesenteric resistance arteries. The pA_2 for FE 205030 (9.3 ± 0.1, mean ± standard

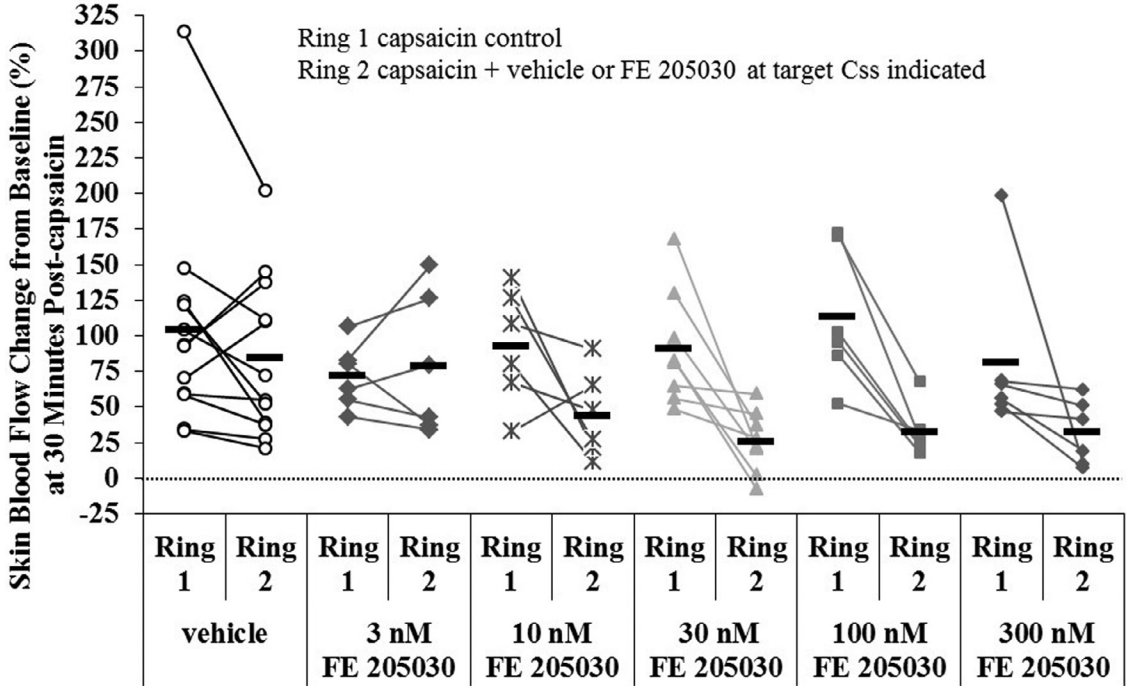

Figure 12. Effect of vehicle or FE 205030, on skin blood flow at 30 minutes post-capsaicin in the cynomolgus monkey CIDV model. Percent change from baseline in Skin Blood Flow at the site of capsaicin application as determined by LDI. Shown are paired measurements in Ring 1 (capsaicin + vehicle for all treatment groups) and Ring 2 (capsaicin + vehicle, FE 205030 at the indicated target Css) from 6-12 replicates per treatment group. Bars indicate Ring 1 and Ring 2 mean for each treatment group.

error, N = 4) was increased relative to telcagepant (8.1 ± 0.2, N = 3), similar to MK-3207 (9.4 ± 0.1, N = 5), and decreased relative to that of olcegepant (10.7 ± 0.3, N = 6) in this study. FE 205030, olcegepant, MK-3207, and telcagepant all exhibited competitive antagonistic behaviour with no observed depression of the αCGRP E_{max} in antagonist-treated arterial segments relative to the paired-control segments.

The in vitro potency and selectivity data (not reported in this paper) indicate that FE 205030 has a very favorable molecular pharmacology profile: IC_{50} of 0.2 nM and >100,000 fold against hAM1R and >6363 fold against hAM2R tested in Human CGRP, AM1R and AM2R receptor cAMP assay using time-resolved fluorescence resonance energy transfer for antagonist potency determination in HEK cells stably overexpressing the respective receptors.

Monkey skin blood flow PD assessment

Under the conditions used in this study, the novel peptidic CGRP receptor antagonist FE 205030 at FE 205030 target Css of 10–300 nM significantly inhibited increases in dermal blood flow induced by the topical application of capsaicin to the forearm of cynomolgus monkeys.

Pharmacokinetics, allometry, human dose prediction and duration of anticipated effect

The rodent PK data indicates that FE 205030 has superior PK properties when compared to the comparator molecules (FE 992325 and 992326). The differences in SC bioavailability's and the superiority of FE 205030 is most likely due to the modifications in positions 1, 2 and 4 in the structure of FE 205030. The substitutions in these positions most likely provide better SC proteolytic stability than those in FE 992325 (which has a similar architecture to FE 205030). Since we did not deeply investigate the SC metabolites for FE 992325, we are unable to assign exact metabolic soft-spots and the resulting stabilization of our clinical candidate FE 205030. The high clearance and low rat SC bioavailability of FE 992326 is explained by the fact that it is an unprotected linear peptide which can be hydrolyzed by many proteases, the most important of them would be trypsin-like enzymes (e.g. tryptase and aminopeptidases). This superior SC bioavailability of FE 205030 is also observed in minipigs, where the bioavailability is ~100% and all indications are that this property will translate and result in a robust exposure in humans.

As discussed in the results section, estimation of human PK parameters (human clearance is expected to be close to the observed minipig clearance of 1.3 ml/kg/min) permitted reasonable confidence in the simulation of human SC PK exposure (Fig. 9). It is hence predicted that at a dose of 0.12–0.4 mg/kg (or a dose of 10–30 mg/day/70 kg human) unbound plasma concentrations are likely to be higher than anticipated free plasma effective concentrations of 30–100 nM, for the required duration of 8 h (which is postulated to reduce chances of migraine recurrence). As described in the previous section, the estimate of effective concentration is derived from the observations presented in Figs. 11 and 12, where at exposures of 30-100 nM of FE 205030 provides a statistically significant complete blockade of capsacin induced dermal vasodilation in cynomolgus monkeys. Thus, it is reasonable to conclude that a self-injectable, convenient and low dose therapy with an optimal duration of action for preventing migraine recurrence is possible with the discovery of FE 205030.

Conclusion

In conclusion, migraine is a debilitating and widespread CNS disease and CGRP antagonists of all modalities (biologics, small molecule and peptide therapeutics), each with their distinct therapeutic potential, can help address a significant unmet medical need. The profile of the peptidic clinical candidate FE 205030 presents a unique opportunity/molecule with ideal PK/PD and pharmaceutical properties and

the potential to be a first in class injectable fast acting selective and potent agent for the treatment of acute episodic migraine.

References

1. Amara SG, Jonas V, Rosenfeld MG, Ong ES, Evans RM. Alternative RNA processing in calcitonin gene expression generates mRNAs encoding different polypeptide products. *Nature*. 1982;298:240–244.
2. Russell FA, King R, Smillie S-J, Kodji X, Brain SD. Calcitonin gene-related peptide: physiology and pathophysiology. *Physiol Rev*. 2014;94(4):1099–1142.
3. Amara SG, Arriza JL, Leff SE, Swanson LW, Evans RM, Rosenfeld MG. Expression in brain of a messenger RNA encoding a novel neuropeptide homologous to calcitonin gene-related peptide. *Science*. 1985;229:1094–1097.
4. Morris HR, Panico M, Etienne T, Tippins J, Girgis SI, MacIntyre I. Isolation and characterization of human calcitonin gene-related peptide. *Nature*. 1984;308:746–748. 1984.
5. Mulderry PK, Ghatei MA, Bishop AE, Allen YS, Polak JM, Bloom SR. Distribution and chromatographic characterisation of CGRP-like immunoreactivity in the brain and gut of the rat. *Regul Pept*. 1985;12:133–143.
6. Weston C, Winfield I, Harris M, et al. Receptor Activity-modifying Protein-directed G Protein Signaling Specificity for the Calcitonin Gene-related Peptide Family of Receptors. *The Journal of Biological Chemistry*. 2016;291(42):21925–21944.
7. McLatchie LM, Fraser NJ, Main MJ, Wise A, Brown J, Thompson N, et al. RAMPs regulate the transport and ligand specificity of the calcitonin-receptor-like receptor. *Nature*. 1998;393:333–339.
8. Brain SD;, Williams TJ, Tippins JR, Morris HR, MacIntyre I. Calcitonin gene-related peptide is a potent vasodilator. *Nature*. 1985;313:54–56.
9. Goadsby PJ, Edvinsson L, Ekman R. Vasoactive peptide release in the extracerebral circulation of humans during migraine headache. *Ann Neurol*. 1990;28:183–187.
10. Lassen LH, Haderslev PA, Jacobsen VB, Iversen HK, Sperling B, Olesen J. CGRP may play a causative role in migraine. *Cephalalgia*. 2002;22(1):54–61.
11. Tepper SJ. History and Review of anti-Calcitonin Gene-Related Peptide (CGRP) therapies: from translational research to treatment. *Headache*. 2018;58:238–275.
12. Amara SG, Jonas V, Rosenfeld MG, Ong ES, Evans RM. Alternative RNA processing in calcitonin gene expression generates mRNAs encoding different polypeptide products. *Nature*. 1982;298:240–244.
13. Edvinsson L. Functional role of perivascular peptides in the control of cerebral circulation. *Trends Neurosci*. 1985;8:126–131.
14. Bell IM. Calcitonin gene-related peptide receptor antagonists: new therapeutic agents for migraine. *J Med Chem*. 2014;57(19):7838–7858.
15. Diener HC, Barbanti P, Dahlöf C, Reuter U, Habeck J, Podhorna J. BI 44370 TA, an Oral CGRP antagonist for the treatment of acute migraine attacks: results from a phase II study. *Cephalalgia*. 2011;31(5):573–584.
16. Recober A, Russo AF. Olcegepant, a non-peptide CGRP1 antagonist for migraine treatment. *IDrugs*. 2007;10(8):566–574.
17. Marcus R, Goadsby PJ, Dodick D;, Stock D; Manos G, Fischer TZ. BMS-927711 for the acute treatment of migraine: a double-blind, randomized, placebo controlled, dose-ranging trial. *Cephalalgia*. 2014;34(2):114–125.
18. Mitsikostas DD;, Reuter U. Calcitonin gene-related peptide monoclonal antibodies for migraine prevention: comparisons across randomized controlled studies. *Curr Opin Neurol*. 2017;30:272–280.
19. Walter S, Bigal ME. TEV-48125: a review of a monoclonal CGRP antibody in development for the preventive treatment of migraine. *Current Pain Headache Rep*. 2015;19(3):6.
20. Durham PL, Vause CV. CGRP receptor antagonists in the treatment of migraine. *CNS Drugs*. 2010;24(7):539–548.
21. Vecsei L, Szok D, Csati A, Tajti J. CGRP antagonists and antibodies for the treatment of migraine. *Expert Opin Investig Drugs*. 2015;24(1):31–41.
22. Olesen J, Diener H-C, Husstedt IW, et al. Calcitonin gene-related peptide receptor antagonist BIBN 4096 BS for the acute treatment of migraine. *N Engl J Med*. 2004;350:1104–1110.
23. Tepper SJ, Cleves C. Telcagepant, a calcitonin gene-related peptide antagonist for the treatment of migraine. *Curr Opin Investig Drugs*. 2009;10(7):711–720.
24. Yuan H, Lauritsen CG, Kaiser EA, Silberstein SD. CGRP monoclonal antibodies for migraine: rationale and progress. *BioDrugs*. 2017;31:487–501.
25. Rist B, Entzeroth M, Beck-Sickinger AG. From micromolar to nanomolar affinity: a systematic approach to identify the binding site of CGRP at the human calcitonin gene-related peptide 1 receptor. *J Med Chem*. 1998;41(1). 1117-2.
26. Rubio-Beltran. Is selective 5-HT 1F receptor agonism an entity apart from that of the triptans in antimigraine therapy? *Pharmacol. Ther.*. 2018;186:88–97.
27. Han L, Liu Y, Xiong H, Hong P. CGRP monoclonal antibody for preventive treatment of chronic migraine: an update of meta-analysis. *Brain Behav*. 2019;9:e01215.
28. Lang M, De Pol S, Baldauf C, Hofmann HJ, Reiser O, Beck-Sickinger AG. Identification of the key residue of calcitonin gene related peptide (CGRP) 27-37 to obtain antagonists with picomolar affinity at the CGRP receptor. *J Med Chem*. 2006;49(2):616–624. 26.
29. Miranda LP, Holder JR, Shi L, et al. Identification of potent, selective, and metabolically stable peptide antagonists to the calcitonin gene-related peptide (CGRP) receptor. *J. Med. Chem.*. 2008;51(24):7889–7897.
30. Yan LZ, Johnson KW, Rothstein E, et al. Discovery of potent, cyclic calcitonin gene-related peptide receptor antagonists. *J Pept Sci*. 2011;17(5):383–386.
31. Tfelt-Hansen P, De Vries P, Saxena PR. Triptans in Migraine A comparative review of pharmacology, pharmacokinetics and efficacy. *Drugs*. 2000;60(6):1259–1287.
32. Smith DA, Di L, Kerns H. The effect of plasma protein binding on in vivo efficacy: misconceptions in drug discovery. *Nature Rev Drug Discov*. 2010;9:929–939.